Resources, Conservation & Recycling 227 (2026) 108741

Contents lists available at ScienceDirect

Resources, Conservation & Recycling

journal homepage: www.sciencedirect.com/journal/resources-conservation-and-recycling

Material composition trends in printed circuit boards of mobile phones

Aleksander Jandric [a,*], Lukas Ginzinger [a], Dzeneta Vrucak [b], Damien Latacz [b], Kathija Shaik [c], Tim Gießmann [b], Ricardo Gabbay de Souza [d], Cledwyn Mangunda [c], Alexander Birich [b], Stefan Salhofer [a]

[a] Institute of Waste Management and Circularity, Department of Landscape, Water and Infrastructure, University of Natural Resources and Life Sciences, Vienna, Muthgasse 107, Vienna, 1190, Austria
[b] Institute of Process Metallurgy and Metal Recycling IME, RWTH Aachen University, Intzestraße 3, Aachen, 52056, Germany
[c] Hydrometallurgy Research Group, Department of Chemical Engineering, University of Cape Town, Private Bag X3, Rondebosch, 7701, South Africa
[d] Department of Environmental and Resource Engineering, Technical University of Denmark, Kongens, Lyngby, 2800, Denmark

ARTICLE INFO

Keywords:
Smartphones
Precious metals
Decreasing metal content
Printed circuit boards
Portable X-ray fluorescence (pXRF)
Material composition trends
Recycling

ABSTRACT

In this research, we have investigated 45 mobile phones manufactured between 1998 and 2021. After dismantling, the resulting Printed Circuit Boards (PCBs) have been mechanically processed and homogenised. From each PCB, three sample pellets were created and analysed with a portable X-Ray Fluorescence (pXRF). In addition, a post-hoc calibration was performed to correct element and sample-specific biases. This approach allowed us to analyse a large sample size and to identify element mass value trends over time. The results for precious metals show an average annual decrease -2.49 mg/PCB for Ag, -1.14 mg/PCB for Au, and -0.13 mg/PCB for Pd. By contrast, the concentrations of Cu and Ni were increasing, but due to the decreasing mass of PCBs, the overall trends remained constant. Ultimately, the applied methodological approach was effective for analysing large number of samples and provided unique insights into the material trends across different generations of mobile phones.

1. Introduction

Mobile cellular subscriptions have sharply increased from 91 million in 1995 to 8.9 billion in 2023, corresponding to approx. 1.1 mobile cellular subscription per person worldwide (ITU, 2024; Worldometers, 2025). Each mobile cellular subscription requires at least one functioning mobile phone for use. While the average mass of smartphones varies by model, this can be simplified by estimating the average mass of a smartphone to be around 140 g (Bonov, 2018). As these devices supporting the 8.9 billion mobile subscriptions become obsolete, they are expected to generate approx. 1.22 million tonnes of electronic waste. The sheer volume of this waste stream and its complex material composition can lead to harmful effects on human health and pose a significant environmental burden due to improper disposal and recycling practices (Cesaro et al., 2019; Owusu-Sekyere et al., 2024; Vaccari et al., 2019).

The functional versatility of a mobile phone is mirrored in the material complexity of its components, such as camera, touch-screen display, battery, and others. The Printed Circuit Board (PCB) represents the core component for operating the different functions of a mobile phone and has the most complex material composition compared to all other components. The metal fraction of PCBs consists of base metals, e.g., copper (Cu), iron (Fe), nickel (Ni), tin (Sn), and zinc (Zn), precious metals, e.g., silver (Ag), gold (Au), palladium (Pd), rare and critical metals, e.g., indium (In), gallium (Ga), and germanium (Ge), and toxic heavy metals, e.g., lead (Pb), mercury (Hg), cadmium (Cd), and arsenic (As) (Bookhagen et al., 2018; Holgersson et al., 2018; Kasper et al., 2011; Oguchi et al., 2011). The economic value of base and precious metals is the main driving force behind the development of PCB recycling technology (Liu et al., 2023). On the other hand, the toxic heavy metals and organic pollutants pose the significant health and environmental risks resulting from inadequate, informal recycling practices (D'Adamo et al., 2019).

Different models and manufacturers contribute to the compositional variability of PCBs in mobile phones. Currently, no standardized methods exist for their characterization to effectively support value recovery operations (Van Yken et al., 2021). At the laboratory scale, the elemental composition of a sample can be determined by dissolving the

* Corresponding author.
E-mail address: aleksander.jandric@boku.ac.at (A. Jandric).

https://doi.org/10.1016/j.resconrec.2025.108741
Received 21 May 2025; Received in revised form 24 October 2025; Accepted 4 December 2025
Available online 11 December 2025

material in highly potent acids, such as aqua regia, before applying spectroscopic techniques such as atomic absorption spectroscopy (AAS) or inductively coupled plasma atomic emission spectroscopy (ICP-OES). The digestion of PCBs can be slow and challenging, with potential inconsistencies from material inhomogeneity, incomplete digestion, or analyte loss through volatilization or precipitation (Lancaster et al., 2024).

Among the bulk-representative analytical methods, neutron-based techniques such as instrumental neutron activation analysis (INAA), in-beam neutron activation analysis (in-beam NAA) and prompt-gamma neutron activation analysis (PGAA) are effective for determining the elemental composition of PCBs (Buczkó et al., 2024). These highly sensitive techniques enable the simultaneous detection of elements in complex samples without the need for digestion. However, despite their potential, the high cost per analysis and the limited number of laboratories equipped with these instruments remain a challenge (Buczkó et al., 2024). In addition, X-ray fluorescence spectroscopy (XRF) serves as a non-destructive technique for elemental analysis of PCBs, with portable versions (pXRF) enhancing accessibility for field applications. Although it has limited sampling depth and is not suitable for coarser samples, semi-quantitative results can still be obtained by calibrating the XRF using a fundamental-parameter calibration (Lancaster et al., 2024).

As shown above, the PCB is a complex recyclable material stream that presents different recycling challenges due to its composition. Over the last 25 years, many patents have been published on PCB recycling, ranging from dismantling, shredding and milling, hydrometallurgical and pyrometallurgical processes (Rocchetti et al., 2018). Despite the different research approaches, only pyrometallurgical processes have been established on an industrial scale. An overview of leading global recycling processing companies is provided in Table 1. However, the recycling processes described in the table cannot process 100 % waste PCB input material, without pre-treatment or specialized furnaces, but require integration of waste PCBs into the copper converter/smelter process. A detailed description of the integrated copper processing can be found in (Pawlek, 1983). Although the general recycling concept is the same, the recovered valuable metals differ significantly depending on the company's specific recycling chain and more precise and faster analysis methods could help improve recycling efficiencies. An overview of leading metallurgical WEEE recycling companies is shown in Table 1.

Even though a number of scientific publications have been published regarding the material composition screening of PCBs using XRF methodology (Gómez et al., 2023; Ippolito et al., 2021; Korf et al., 2019; Otsuki et al., 2020), to the best of our knowledge, no XRF analytical protocol is available that offers methodological improvement to

Table 1
Overview of leading metallurgical WEEE recycling companies.

Industrial process	Metals recovered	Integration in Copper route (PCB Quota [%])	Source
Umicore	Ag, Au, Pt, Od, Rh, Ir, Ru, Pb, Cu, Ni, Sb, Se, In, Te, As	Smelter (6,4%)	(Hagelüken, 2006)
Glencore	Cu, Au, Ag, Pt, Pd, Se, Te, Ni	Smelter (N/A*)	(Themelis et al., 1972) (Khaliq et al., 2014)
LS-Nikko Copper	Cu, Au, Ag, Se, Te, Pd, Pt, Ni, Bi	Smelter (N/A*)	(Oh et al., 2012)
Aurubis AG	Cu, Ni, Sn, Pb, PGM, Au, Ag, Zn, Sb	Smelter (15 – 20%)	(Nolte, 2018)
Boliden	Au, Ag, Se, PGM, Cu, Ni	Kaldo Reactor (100%), Converter	(Lennartsson et al., 2018)
DOWA Japan	Au, Ag, Cu, Pb, Bi, Se, Te, In, Ga, Sb, PGM, Zn Sn, Ni	Smelter (up to 100 % with pretreatment)	(DOWA, 2024) (Naka, 2006)

[*] No Data Available.

enhance the reliability of XRF metal content analyses. In this research, a precise manual dismantling procedure was performed to obtain a comprehensive insight into mobile phone components and their change in mass over time. In the next step, PCBs were mechanically pulverised, homogenised, and screened for material composition using pXRF. A novel post hoc calibration for pXRF, as described by Jandric et al. (2024), combined with the generation of method-specific sample pellets, significantly improved the accuracy of pXRF analysis. This approach enabled the analysis of a large sample set and consequently a detailed trends analysis of PCB material composition.

2. Experimental

2.1. Description of the sample set

A sample set encompassing 45 different used mobile phones was randomly collected at a charity hub of second-hand shops in Vienna, Austria. The sampled mobile phones were organised according to the manufacturer, model, and first release date and then labelled with a specific sample ID. The mobile phone sample set was categorised into two groups: feature phones ($n = 18$) and smartphones ($n = 27$). Feature phones are defined as mobile phones operated mainly by physical keyboards without third-party applications. Smartphones are defined as mobile phones operated by touchscreens and possessing developed internet access capabilities in combination with third-party applications. A complete list of sampled mobile phones is shown in Table S 1, Supplementary Material.

2.2. Manual dismantling

Each mobile phone was manually dismantled using a mobile phone repair toolkit. Dismantling process started with opening the back cover casing and removing the mobile phone battery. Next, screwdrivers and spudger were used to open the front casing and mainframe. The feature phone components are assembled by mechanical clips and screws and connected by insulated and non-insulated copper wires, which makes their dismantling and classification significantly simpler compared to the smartphones. Smartphone components, primarily the battery and touchscreen display, are often glued to other components or the mainframe. Consequently, the dismantling of smartphones requires using a hot air heat gun and suction cups to achieve complete separation without damaging the components.

The final step of the dismantling process consisted of the dismantling of components and parts from the mobile phone PCB, which included disconnecting of insulated and non-insulated copper wires, removal of all larger steel parts and screws, and dismantling of the camera, speaker, vibration and other modules. The result represents the mobile phone PCB without further components and materials. This discriminatory definition of what constitutes a mobile phone PCB follows the same principle as determined by Bookhagen et al. (2018), since it enables the direct comparison between different mobile phone models. The resulting components have been classified into 15 categories and weighed with A&D FA-200 laboratory scale (A&D Ltd., Tokyo,Japan).

2.3. PCB sample preparation for pXRF analysis

The mobile phone PCBs resulting from the manual dismantling were handled separately as individual samples for mechanical preparation for material composition analysis with portable X-Ray Fluorescence (pXRF). Mechanical preparation started with cutting a PCB into 2–4 cm large pieces with pliers for metal. Afterward, the PCB fragments were shredded in the Retsch SM 2000 mill (Retsch GmbH, Haan, Germany) to a particle size <10 mm. In the last step, the shredded PCB were milled in the centrifugal mill Retsch ZM 200 (Retsch GmbH, Haan, Germany) to a particle size <500 µm. The resulting PCB powder was homogenised by shaking and stirring within the 100 mL HDPE wide-neck jars with screw caps. In the next step, three random samples with an average mass of ~1 g were taken from milled PCB using stainless steel laboratory spoon and pressed into sample pellets using hydraulic press. The press applied a force of around 10 tons (~98 kN), which was sufficient to produce stable PCB sample pellets without the need for additional fixing reagents.

2.4. XRF analysis and post hoc calibration

To analyse the material composition of mobile phone PCBs with pXRF in this study, we followed the methodology and post hoc calibrations principle published in Jandric et al. (2024). The sample pellets, three per mobile phone, prepared from milled PCBs were analysed by pXRF Niton XL3t Ultra Handheld XRF Analyser (Thermo Scientific Portable Analytical Instruments Inc., Tewksbury, USA) in a Niton 430–032 Mobile Test Stand Assembly. The sample pellets were measured in triplicates on both sides (six measurements total per pellet) for 100 s using the 'Environmental mode' program of the pXRF device, in filter configuration 60 s (main), 20 s (low), and 20 s (high).

This approach allows for a more accurate and reliable determination of the material composition of mobile phone PCBs. For the pXRF post hoc calibration, calibration aliquots have been created by combining the Certified Reference Material (CRM) BAM-M505a 'Electronic Scrap' (Bundesanstalt für Materialforschung und -prüfung, Germany) with virgin polyoxymethylene (POM). The concentrations, uncertainty, and coefficient of variance (CV) of the CRM provided by the producer are available in Table S 2, Supplementary Material. The summary of precision and reliability of conducted post hoc calibrations for elements contained in the CRM are shown in Tables S3 and S4, Supplementary Material.

2.5. Calculation of element concentrations, mass values, and trends for calibrated and uncalibrated elements

Results of pXRF material composition analysis were assessed to determine both element concentration and mass value in mobile phone PCBs. Element concentration refers to the mass fraction of an element, expressed as ppm (mg/kg) for calibrated elements and as arbitrary units (a.u.) for pXRF meta-concentrations for uncalibrated elements. Mass value refers to the absolute mass of an element per individual PCB, expressed as milligrams per PCB (mg/PCB) for calibrated elements and as arbitrary units per PCB (a.u./PCB) for uncalibrated elements.

For each pellet, the arithmetic mean element concentration (in ppm or a.u.) was calculated from the six pXRF measurements. The mean concentration (in ppm or a.u.) of the three pellet means was then calculated for each PCB. For calibrated elements, this was multiplied by the PCB mass (in g) and divided by 1000 to obtain the mass value in milligrams per PCB (mg per PCB). For uncalibrated elements, the mean concentration (a.u.) was multiplied by the PCB mass (g) to obtain the mass value (a.u. per PCB). The element mass value for each of the 45 mobile phone PCBs was calculated using following Eq. (1):

$$Q_{X,k} = \left(\frac{1}{m}\right) \times \left(\frac{1}{n}\right) \times \left(\sum_{i=1}^{m} \sum_{j=1}^{n} X_{i,j,k}\right) \times \left(\frac{mPCB_k}{1000}\right) \quad (1)$$

Where

$Q_{X,k}$	=	Quantity of element X in the kth PCB (mg/PCB)
$X_{i,j,k}$	=	pXRF measurement of element X for pellet I, measurement j, on PCB k in ppm (mg/kg)
$mPCB_k$	=	Mass of the kth PCB (g)
k	=	PCB index (1 to 45)
i	=	Pellet index (1 to 3)
j	=	pXRF Measurement index (1 to 6)
m	=	Number of pellets per PCB ($m = 3$)
n	=	Number of pXRF measurements per pellet ($n = 6$)

2.6. Uncertainty calculations

Uncertainty calculations of element concentrations for calibrated elements were calculated following the Guide to the Expression of Uncertainty in Measurement JCGM 100:2008 (JCGM, 2010). The uncertainty calculations were performed separately to obtain analytical, sampling, calibration, and a combined uncertainty of the first three.

The analytical uncertainty ($u_{analytical}$) is calculated to quantify the uncertainty arising from variations in the pXRF measurement process, such as instrument noise, sample positioning, and similar measurement process related variations. It is calculated as the pooled standard deviation (SD_{within}) of the 6 measurements for each of the 3 pellets per mobile phone PCB, divided by the square root of the total number of measurements using the following Eq. (2) per JCGM 100:2008 (JCGM, 2010). The results of analytical uncertainty ($u_{analytical}$) calculations for calibrated and uncalibrated elements are shown in Tables S 17 and S 18, Supplementary Material.

$$u_{analytical} = \frac{SD_{within}}{\sqrt{18}} \quad (2)$$

Where

$u_{analytical}$	=	Analytical uncertainty
SD_{within}	=	$\sqrt{\frac{(n_1 - 1)s_1^2 + (n_2 - 1)s_2^2 + (n_3 - 1)s_3^2}{n_1 + n_2 + n_3 - 3}}$
s_i	=	Standard deviation of 6 measurements for pellet i ($i = 1, 2, 3$)
n_i	=	Measurements per pellet (df = 5, total df = 15)

The sampling uncertainty ($u_{sampling}$) was calculated to quantify the mean concentration uncertainty of an element based on the variability between the sample pellets for each mobile phone PCBs. The observed variability arises from heterogeneity of element dispersion in the pulverised PCB sample pellets. It was calculated as the standard deviation of the three pellet medians divided by the square root of the number of pellets, using the Eq. (3) per JCGM 100:2008 (JCGM, 2010). The results of sampling uncertainty ($u_{sampling}$) calculations for calibrated and uncalibrated elements are shown in Tables S 19 and S 20, Supplementary Material.

$$u_{sampling} = \frac{SD(w_1, w_2, w_3)}{\sqrt{3}} \quad (3)$$

Where

$u_{sampling}$	=	Sampling uncertainty
SD	=	Standard deviation
w_i	=	Mean pellet concentration of six measurements

The calibration uncertainty ($u_{calibration}$) quantifies the variability in median concentration values arising from the calibration curve used to convert pXRF signals to concentration for individual elements. The uncertainty arises due to the goodness-of-fit of linear regression models, limitations of the calibration slope, intercept, and residual variability of other calibration parameters. It is calculated for the element's mean concentrations for each sample pellet following the Eq. (4) per JCGM 100:2008 (JCGM, 2010). Uncalibrated elements do not have a model fit to contribute to the calibration uncertainty and are therefore excluded from this calculation. The results of calibration uncertainty ($u_{calibration}$) calculations are shown in Table S 21, Supplementary Material.

$$u_{calibration} = \sqrt{\left(\frac{s_{res}}{\sqrt{n_{cal}}}\right)^2 + (u_a \times x_i)^2 + u_b^2} \quad (4)$$

Where

$u_{calibration}$	=	Calibration uncertainty
s_{res}	=	Residual standard error (ppm)
n_{cal}	=	Number of calibration points
u_a	=	Slope standard error (ppm/% Certified Reference Material)
x_i	=	Predictor value (%Certified Reference Material)
u_b	=	Intercept standard error (ppm)

Subsequently, the previous three types, i.e., analytical, sampling, and calibration uncertainty, have integrated under the combined uncertainty ($u_{combined}$) to quantify the total uncertainty in the mean concentration of an element per mobile phone PCB. The separately calculated uncertainties are assumed to be independent as they arise from distinct sources, i.e., measurement noise, sample heterogeneity, and calibration regressions. The combined uncertainty is calculated as the square root of the sum of squared uncertainties following the Eq. (5) per JCGM 100:2008 (JCGM, 2010):

$$u_{combined} = \sqrt{u^2_{analytical} + u^2_{sampling} + u^2_{calibration}} \tag{5}$$

The mass value uncertainty (u_{mass}) was calculated to quantify the uncertainty in the absolute mass (in mg) of an element in a given mobile phone PCB, based on the element concentration (in ppm) and PCB mass (in g). Since the divergence in PCB mass was negligible due to low divergence of the laboratory scale, simplified approach using the combined uncertainty from concentrations was used following the Eq. (6) per JCGM 100:2008 (JCGM, 2010):

$$u_{mass} = \frac{u_{combined} \times m}{1000} \tag{6}$$

Where

u_{mass}	=	Mass value uncertainty
$u_{combined}$	=	Combined uncertainty from element concentration (ppm)
m	=	Mass of individual PCB (g)

2.7. Data analysis and statistical methods

The datasets consisting of total masses of mobile phones, masses of individual components, and material composition between individual PCBs have a generally non-normal right-skewed distribution. For this reason, the median was chosen over the arithmetic mean as a more accurate representation of central tendencies, and non-parametric tests have been applied for comparisons between feature phones and smartphones. Consequently, Kruskal-Wallis tests were used to test the difference in median mass of components and element concentrations between feature phones and smartphones. Spearman's rank correlation coefficient was applied to test the correlation between relative element concentrations in mobile phone PCBs.

A trend analysis was conducted to assess the changes in the mass of mobile phone components, changes in the mass value of calibrated elements, and changes in composition trends of uncalibrated elements, in relative terms between pXRF meta-concentrations between different PCBs. Linear regression was employed for this analysis, with the year of manufacture as the predictor variable and the respective element concentrations as response variables. In addition, power analysis was conducted to determine whether the sample size consisting of 45 mobile phone PCBs manufactured between 1998 and 2020 is sufficient to detect trends in respective element concentration changes over time. The specific conditions of the sample size test included the null hypothesis (H_0): the slope of element content is zero, and alternative hypothesis (H_1): the element content changes over time, at the significance level $\alpha = 0.05$ for two-tailed test and desired statistical power $1–\beta = 80$ %.

The sample size analysis assessed the number of mobile phone PCBs required to detect a significant linear regression slope (β_1) for trends in element mass values (mg per PCB) over time, residual standard deviation in mg/PCB (σ_y), and standard deviation of the predictor (σ_x, years) which represents the variability in the year of manufacture across the 45 PCBs. The sample size sufficiency was assessed using the following Eq. (7):

$$n = \frac{\left(Z_{1-\alpha/2} + Z_{1-\beta}\right)^2 \times \sigma_y^2}{\beta_1^2 \times \sigma_x^2} \tag{7}$$

Where

α	=	0.05 (two-tailed)
$Z_{1-\alpha/2}$	=	1. 959,964
$Z_{1-\beta}$	=	0. 8416,212
σ_x	=	6.431457
n	=	Number of individual mobile phone PCBs ($n = 45$)

3. Results

3.1. Comparison of mobile phone components

The total mass of mobile phones was slightly decreasing until approximately 2008–2010, but since the transition to smartphones, the trend has reversed and the total mass has been steadily increasing since then. Fig. 1 shows the total mass distribution and chronological breakdown of the year of manufacture. A full list of components resulting from manual dismantling is available in Table S 5, Supplementary Material. The results of manual dismantling show that the mass of components in feature phones was more evenly distributed across different categories. In contrast, only four out of fifteen components, i.e., the battery (35.56 ± 10.83 g), display (33.15 ± 7.18 g), mainframe (24.69 ± 12.45 g), and casing (17.38 ± 12.94 g), account for 83 % of the total mass of median smartphone (see Fig. S 1, Supplementary Material).

Overall, several notable trends in mobile phone components have been observed. Keyboards have been phased out as a component with touch screens filling in as a replacement. In addition, newer smartphones first manufactured since 2017, contain two new components: a Taptic engine and a Qi-charging module. Taptic engine provides haptic feedback technology, allowing devices to create "tactile sensations that mimic physical buttons. It is made of copper wire coils, magnets, and springs (Kim et al., 2022). The Qi-charging module enables wireless battery charging through an oscillating electromagnetic field and is primarily made up of copper wire coils that transmit energy to the battery (Elmannai et al., 2023).

Over time, PCBs have become significantly lighter (see Fig. 2) and more compact with a higher number and density of mounted integrated circuits, capacitors, and similar PCB components. In addition, processing chips have become larger, while the area and number of gold-plated connectors have been greatly reduced or eliminated. The results of the Kruskal-Wallis tests comparing the median mass of all components from feature phones and smartphones are shown in Table S 6, Supplementary Material. The linear regression models testing the change in components' mass over time is shown in Table S 7, Supplementary Material.

3.2. Element concentrations in mobile phone PCBs

Element concentrations analysis for feature phones and smartphones compares mass fractions (in ppm) of specific elements between individual PCBs. The results of element concentration comparisons are limited to the extent of elements present in the Certified Reference Material (CRM). The results show significant increase in total median metal concentration from 369,111 ppm (37 mass %) in feature phone PCBs to 677,954 ppm (68 mass %) in smartphone PCBs (see Fig. S 2, Supplementary Material). In addition, Cu, Ni, and Sn, constitute substantial share of all screened elements ranging from 35 mass % of feature

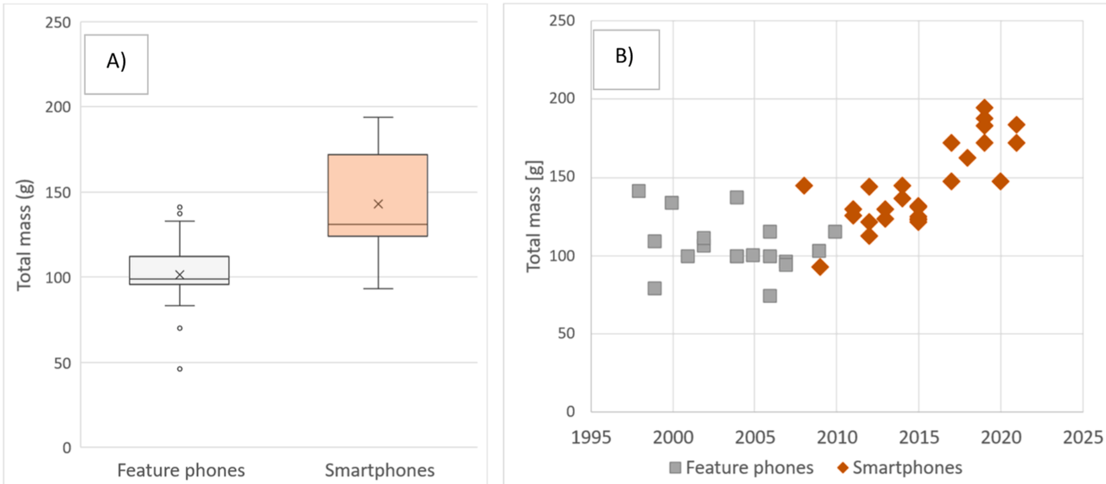

Fig. 1. (A) Comparison of mass distribution per mobile phone before dismantling between feature phones ($n = 18$) and smartphones ($n = 27$) and (B) Total mass distribution trends by year of production.

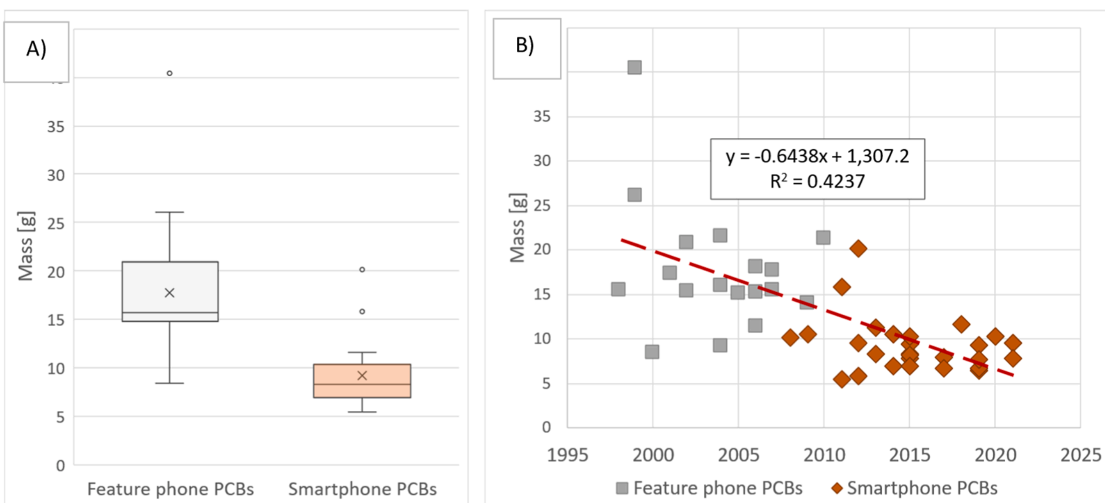

Fig. 2. (A) Shows box plots of PCB masses of PCBs from feature phones and smartphones and (B) Shows PCB masses by year of production.

phone PCBs up to 65 mass % of smartphone PCBs. All other elements, including precious and critical elements, make both in feature phones and smartphones <1 mass % of PCB.

Important to note that Fe, Zn, and Mg are elements that are also present in relatively high concentrations in mobile phone PCBs, but these are not considered in this part of the analyses as they are not part of the CRM. The post hoc calibration adjusted element composition (in ppm) for individual mobile phone PCBs is shown in Table S 8, Supplementary Material. Median differences in element concentrations in PCBs between feature phones and smartphones were tested using Kruskal Wallis tests (Table S 9, Supplementary Material). The results show the most significant change in element concentration was with Cu, whose concentration increased by 86 % from a median of ~320,000 ppm in feature phones to a median of ~ 595,000 ppm in smartphones. Similarly, the concentration of Ni increased by 103 % from ~ 28,000 ppm in feature phone PBCs to ~ 57,000 ppm in smartphone PCBs.

The median concentration of elements Pb, Au, Pd, As, and Cd decreased significantly. The median concentration of Au decreased from 1,244 ppm in feature phone PBCs to 428 ppm in smartphone PCBs, while the median concentration of Pd decreased from 101 ppm in feature phone PBCs to 24 ppm in smartphone PCBs. Boxplot summary of element concentrations (in ppm) comparison between feature phones and smartphones for calibrated elements are shown in Fig. 3, while Kruskal-Wallis test result summaries are shown in Table S 9, Supplementary Material.

Spearman's rank correlation coefficient tests were conducted to test the relationship between different element concentrations within the same type of PCBs, i.e., feature phones and smartphones separately. The results for feature phone PCBs revealed the strongest positive correlations: lead (Pb) with arsenic (As) at 0.72, lead (Pb) with palladium (Pd) at 0.61, and palladium (Pd) with silver (Ag) also at 0.61. The most significant negative correlations in feature phone PCBs were observed between copper (Cu) and cadmium (Cd) at −0.50, and between chromium (Cr) and Pd at −0.52. The test results for smartphones indicate strong positive correlations between several elements: tin (Sn) and palladium (Pd) show a correlation of 0.87 and Sn and silver (Ag) have a correlation of 0.72. There were no clear negative correlations between element concentrations in smartphone PCBs (see Fig S 3, Table S 10 and Table S 11, Supplementary Material).

3.3. Mass values of elements in mobile phone PCBs

To identify and analyse trends in elemental content in PCBs over time, the element concentrations (in ppm) have been multiplied by the

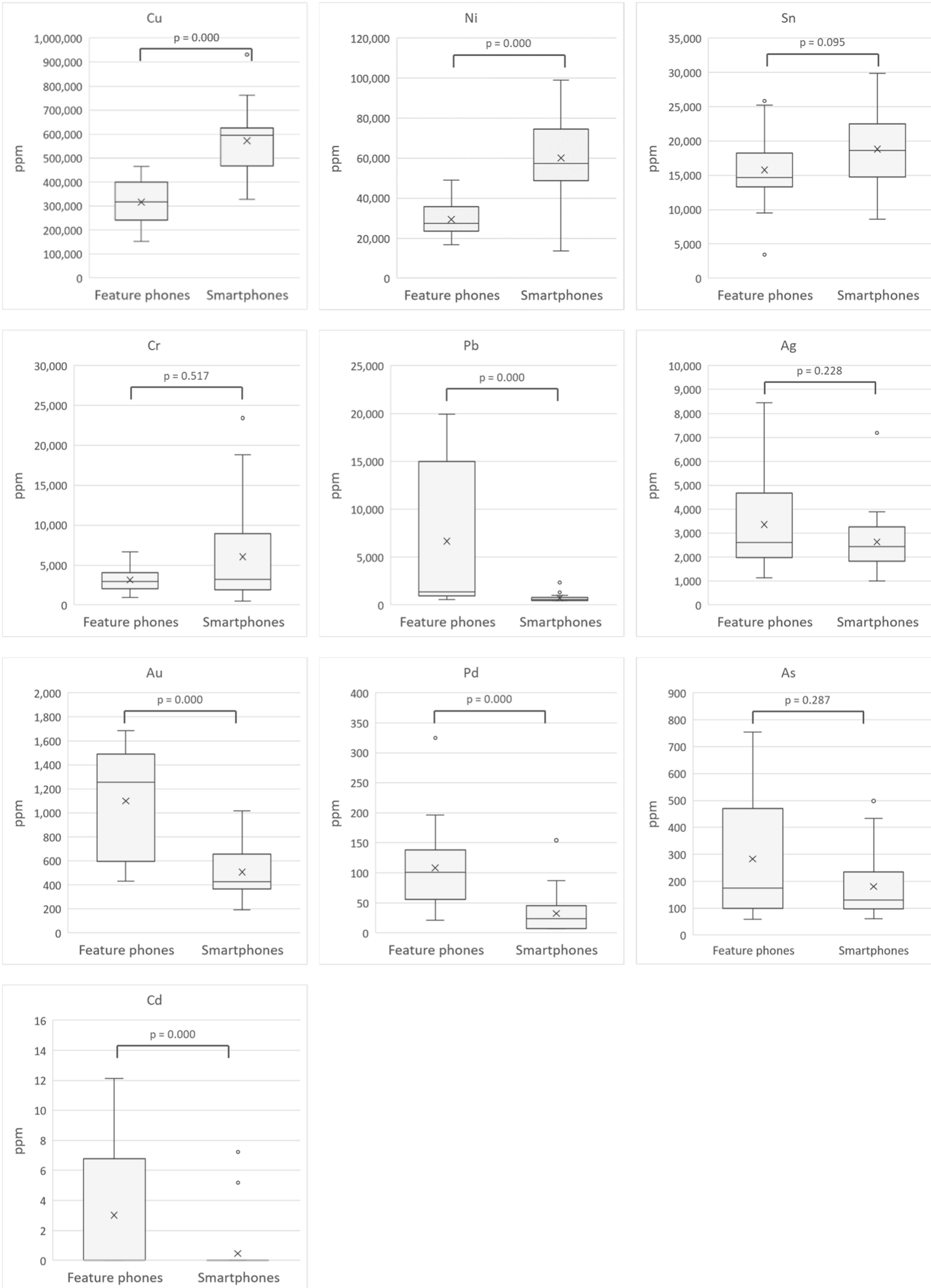

Fig. 3. Comparison of element concentrations (in ppm) in PCBs from feature phones and smartphones, measured by pXRF for calibrated elements, including p-values for the conducted Kruskal-Wallis tests.

mass of PCB to obtain an mass value of an element expressed as mg/ PCBs. The results of the trend analysis for total elemental concentration in mobile phone PCBs remained relatively constant over the considered time period (see Fig S 4, Supplementary Material). This comes as a result of the increasing elemental concentration per PCB (see Fig S 2, Supplementary Material) being offset by the declining mass of PCBs (see Fig. 2). The conducted linear regression analysis of total elemental concentration resulted in a p-value of 0.620, showing that there is no statistically significant correlation.

The sample size analysis was performed across all linear regression models for all calibrated elements. The results indicate that for all elements with clearly observed trends, the sample size of 45 mobile phone PCBs minimal sample size for achieving desired statistical power $1-\beta =$ 80 % has exceeded with significant margin. For example, the required sample sizes for 80 % power in a two-sided test are 10 for Au, 16 for Pd, 22 for Pb, 24 for Ag, and 26 for Sn. The requirement for assessing the trend of Au is particularly consequential, as Au accounts for over 70 % of the total pure metal value in mobile phone PCBs (Bookhagen et al., 2020) and plays decisive role in the recycling process (Romano et al., 2023). The power achieved in assessing the Au trend with a sample size of 45 PCBs is greater than 99 %, ensuring reliable trend detection. A summary of the sample size analysis for all calibrated elements is shown in Table S 12, Supplementary Material.

The results of linear regression models for individual elements show decreasing quantities for most elements. Seven out of ten analysed elements show statistically significant decreasing quantities with p-values

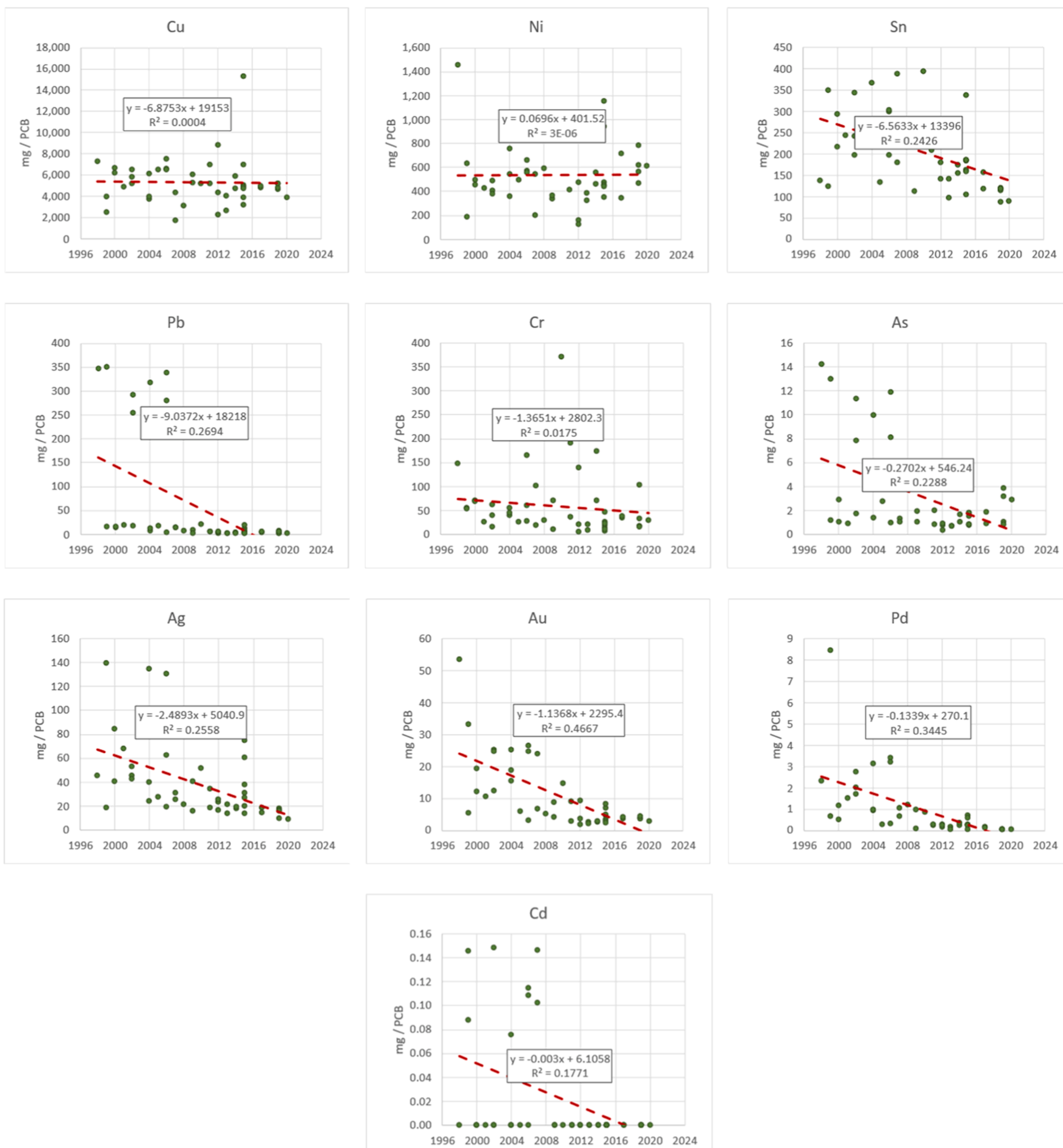

Fig. 4. Trends over time in mass share (in mg) of selected metals in mobile phone PCBs.

<0.05. A particularly strong decrease in quantity per PCBs was observed with elements regulated with the RoHS Directive, i.e., Pb, As, and Cd. However, this decrease was not gradual but abrupt between the years 2005 and 2007. Consequently, these elements show a relatively low coefficient of determination, with R^2 ranging between 0.18 and 0.27. Similar trends were observed with precious metals, where an average annual decrease was −2.49 mg/PCB for Ag, −1.14 mg/PCB for Au, and −0.13 mg/PCB for Pd. Overall, the median Ag content decreased from 44 mg/PCB in feature phones to 19 mg/PCB in smartphones. The decline in gold content is even more pronounced, with a median of 19 mg/PCB in feature phones compared to just 4 mg/PCB in smartphones.

The mass value of Cu and Ni remained constant over time with a median content of approx. 5200 for Cu and 480 mg/PCB for Ni, without significant differences between feature phones and smartphones. This stability is attributable to an increase in concentration that was balanced by a decrease in the mass of PCBs. Additionally, tin (Sn) also exhibited a statistically significant decreasing trend, where the rising concentration was completely offset by the declining mass of PCBs. The quantity of precious metal significantly decreased over time, with the coefficient of determination R^2 ranging between 0.47 for Au, 0.34 for Pd, and 0.26 for Ag. A graphical summary of linear trend analyses is shown in Fig. 4, while the full list of element mass values (in mg/PCB) is shown in Table S 13 and the overview of linear regression model's results is shown in Table S 14, Supplementary Material.

3.4. Trend analysis for uncalibrated elements in mobile phone PCBs

Beyond the ten metals present both in mobile phone PCBs and in the CRM, trend analysis has been conducted also for a further 20 elements detected by the default 'Environmental mode' program of the pXRF. Since the trend analyses are relying on uncalibrated concentrations, the results are expressed in arbitrary units per Printed Circuit Board (a.u. / PCB) representing uncalibrated pXRF meta-concentrations. The catalogue of uncalibrated element concentrations for individual mobile phone PCBs composition is shown in Table S 15, Supplementary Material.

The trend analysis of uncalibrated elements revealed a negative linear regression slope for 17 of the 20 elements analysed, indicating a decrease in quantities over time. The only two exceptions are Hg, which, with several outliers, is largely absent from printed circuit boards, and iron (Fe), which exhibited an increase in concentration. Overall, the analysis found only a weak correlation between element quantity and the year of production. Notably, calcium (Ca) and scandium (Sc) exhibited a strong relationship with an $R^2 = 0.55$ between the amount in PCB and the year of production. Elements with particularly weak correlation with R^2 below 0.2 are Fe, Zn, Ti, Zr, and Sb. A graphical summary of linear trend analyses for selected elements is shown in Fig. 5, while an overview of the linear regression model's results for uncalibrated elements is shown in Table S 16, Supplementary Material.

4. Discussion

The mobile phone PCBs underwent significant changes since their first introduction to the broader market in mid-1990s. The demand for faster processing speed has led to more compact PCBs with an increasing number, size, and density of mounted components and integrated chips (ELEPCB, 2024; Shearer, 2011). This development, which coincided with the transition from feature phones to smartphones, has led to a more compact PCB architecture.

Manual dismantling of mobile phones is usually the first step in both material composition analysis and recycling. The present research provides a higher dismantling depth than generally found in the literature. Fontana et al. (2019) divided their mobile phone components after dismantling into five categories, focusing on their material composition and presenting average material fractions of all dismantled mobile phones. Singh et al. (2018) provide eight different component categories comparing feature phone and smartphone changes. Bruno et al. (2022) reduced the potential 50 component categories to four categories to reduce complexity.

This research aligns with findings from Bruno et al. (2022), which noted an average weight increase in smartphones alongside a decrease in the weight of their PCBs. The weight differences between feature phones and smartphones are predominately based on the display fraction (Bruno et al., 2022; Kumari and Samadder, 2023). However, the significant decrease in PCB weight in smartphones relative to feature phones is not corroborated by Kumari and Samadder (2023), Gómez

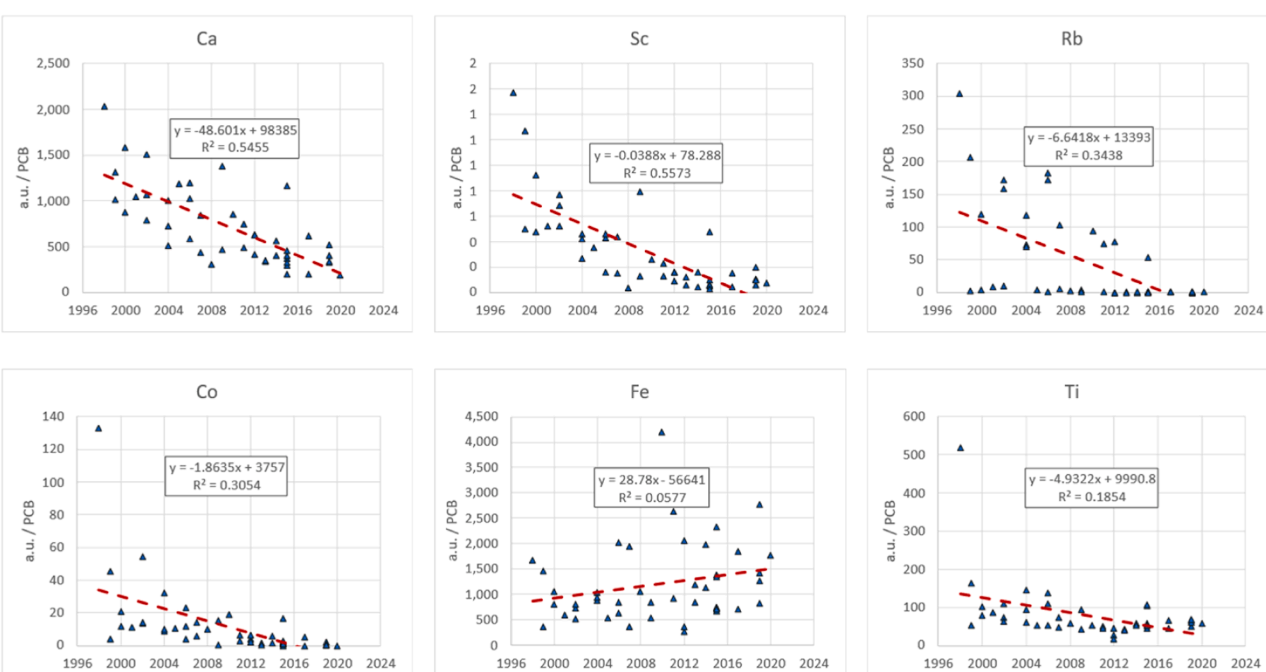

Fig. 5. Trend analysis for selected uncalibrated metals from mobile phone PCBs.

et al. (2023), and Singh et al. (2018). These differing results arise from different methodological approaches used to dismantle mobile phones to obtain PCBs, as there is currently no standardized protocol for this process.

Generally, the material composition screening of PCBs requires meticulous sample preparation and advanced analytical techniques. Consequently, PCBs are usually analysed using microwave-assisted acid digestion in combination with ICP-OES and ICP-MS analytical techniques. While representing the gold standard in analytical chemistry, ICP-OES and ICP-MS are highly time and cost-intensive. This substantially limits the number of samples that can be analysed within any specific research, which, with a few exemptions, usually range between 5 and 10 PCBs (Bookhagen et al., 2020; Gómez et al., 2023; Oguchi et al., 2011; Rao et al., 2021; Zhao et al., 2017). In contrast, material composition screening with X-Ray Fluorescence (XRF) based analytical techniques requires less sample preparation, and the analytical process is remarkably faster than ICP-based analytical techniques. However, XRF material screening results show a substantial lack of accuracy in screening complex samples such as PCBs (Ichikawa et al., 2023; Korf et al., 2019).

Since the early 2000s, there was an overt effort to phase out and replace certain toxic heavy metals, i.e., Pb, Cd^{2+}, Cr^{6+}, and As, driven by the EU Directive on Restriction of Hazardous Substances (EU RoHS), which restricted the use of these elements in electronic appliances. Around the same period, influenced by economic considerations and technological development, the content of precious metals, primarily Au, Pd, and Ag, started to decline. Although the hypothesis that the concentration of precious metals in PCBs is decreasing has been discussed at various scientific and recycling industry conferences, as well as in non-scientific literature (Geyer and Doctori Blass, 2010; Kamczyc, 2021; Workman, 2016), it has not yet been conclusively proven. The variability of mobile phones and PCBs, along with the differing analytical methods used, has rendered direct meta-comparison across various scientific publications not feasible.

A sample set encompassed in this research, was sufficient for a reliable statistical trend analysis of precious metals, achieving a statistical power greater than 97 % for elements Ag, Pd, and Au. Our results, which demonstrate a significant decrease in Au content ($\beta_1 = -1.1368$ mg/PCB*year, at $p < 0.001$), provide, to the best of our knowledge, one of the first statistically proven and quantified confirmations of decreasing trends in the Au content of mobile phone PCBs. These findings are consistent with results published by Tantawi and Hua (2021). Although Singh et al. (2018) did not verify a decrease in silver content, it is important to note that the smartphones they analysed were models from 2006 to 2015. Notably, as illustrated in Fig. 4, silver content varied significantly before 2016, followed by a sharp decline in subsequent years.

The concentration of copper (in ppm) in smartphone PCBs has been shown to increase compared to that in feature phone PCBs, as evidenced by Gómez et al. (2023). This rise can be attributed to higher manufacturing standards and technological advancements in PCB design. The newest PCBs often feature increased copper conductive layers, ranging from a basic six layers to as many as 30 layers. This enhancement is essential for ensuring sufficient electrical conductivity, effective heat dissipation, and better integration of board components (Perdigones and Quero, 2022; Sahan et al., 2019). The increase in Ni concentration might be explained by its increased use for connectors, resistors, shield plates, and other mounted components (Gorewoda et al., 2020).

In the literature, the material composition of mobile phone PCBs is generally represented in relative terms expressed in ppm or mg/kg units, without considering the overall mass of the PCBs. The element composition results (in ppm) in this research align with findings from Gómez et al. (2023). Additionally, the study by Gupta et al. (2021) reported an initial increase in metal share (in ppm) from feature phones to smartphones, consistent with current research, but also reported a decline in smartphone models produced between 2011 and 2016. It's important to note that the smaller sample size in Gupta et al. (2021) limits the ability to establish definitive trends..

Furthermore, we observed several positive and negative correlations between elements. The observed correlations might be explained by the following technological trends:

- Changes in soldering alloys, influenced by the RoHS Directive, led to a transition from tin-lead (Sn-Pb) to tin-silver (Sn-Ag) and other solder alloys (Bieler and Lee, 2017).
- The common combination of Pb and Pd found in multilayer ceramic capacitors (Liu et al., 2020).
- The use of Ni as an underlayer for gold plating in connectors and contacts (Gorewoda et al., 2020)
- The gradual replacement of Au with copper Cu due to advancements in material technology (Zhang et al., 2020).

Based on the results obtained in this research, the evidence indicates that the increasing functionality and computing power of new generation mobile phone PCBs did not lead to increased used of Au. In contrast, the need of Au connector plating was offset by advancements in material technology and consolidation of surface components. The impact of these metals' changes over time on the recycling industry as base metal concentration increases while precious metal concentration decreases is anticipated to require novel, more agile recovery technologies capable of adapting to changing input streams based on the pre-screened material composition. The PCB recycling and recovery technologies of tomorrow will require high operating efficiencies in small-scale and mobile scope, especially in developing countries lacking the raw ores needed for the current capital-intensive and geographically highly concentrated integrated copper smelters (Chen et al., 2019; Maurice et al., 2021). Additionally, evolving recycling practices could have beneficial effects, particularly in light of the increasing emphasis on design strategies that prioritize recyclability and sustainability.

5. Conclusions

This research paper encompasses a detailed analysis of the large sample mobile phones and an assessment of mobile phone components' mass comparison between feature phones and smartphones, as well as components' change in mass over a nearly 25-year time span. Furthermore, the material composition analysis of mobile phone PCBs has been conducted using portable X-ray fluorescence (pXRF) to obtain element concentrations and mass values.

The material composition of PCB has changed significantly over time. Currently, three elements account for about 65 mass % of a median smartphone PCB, while all other analysed elements contribute <1 mass % each of a median smartphone PCB. The median Cu concentration increased by 46 % when comparing feature phones to smartphones, whereas the concentrations of nearly all other elements decreased in smartphones. The relative increase in metal concentration is offset by the decreasing mass of PCBs.

Consequently, the mass value of Cu and Ni (in mg/PCB) remained relatively constant, while the amount of precious metals and hazardous heavy metals regulated by the RoHS directive decreased significantly. The Au content showed particularly sharp decrease from above 20 mg in PCB manufactured around 2000 to <5 mg in PCB manufactured after 2018. Similarly, the amount of Pd decreased from 2–3 mg to <1 mg per PCBs for the same period. As a result, the economic incentive for recycling waste PCBs is diminishing, which may negatively impact the PCB recycling rates.

The pXRF screening of mobile phone PCBs' material composition has also proven helpful for assessing non-calibrated elements by making relative comparisons of the concentration of a target element in one sample to the concentration of the same element in another sample. As a result, the pXRF material screening was able to provide data on 20 additional elements so that it was possible to identify their trends and compare element concentrations of uncommon elements. This capability can be advantageous when screening and evaluating the effectiveness of different recycling and recovery process steps.

CRediT authorship contribution statement

Aleksander Jandric: Writing – review & editing, Writing – original draft, Methodology, Investigation, Funding acquisition, Formal analysis, Data curation, Conceptualization. **Lukas Ginzinger:** Writing – original draft, Investigation, Formal analysis. **Dzeneta Vrucak:** Writing – original draft, Investigation, Conceptualization. **Damien Latacz:** Writing – review & editing, Writing – original draft, Project administration, Funding acquisition. **Kathija Shaik:** Writing – review & editing, Writing – original draft, Conceptualization. **Tim Gießmann:** Writing – review & editing, Writing – original draft, Conceptualization. **Ricardo Gabbay de Souza:** Writing – review & editing, Writing – original draft, Investigation, Formal analysis. **Cledwyn Mangunda:** Writing – review & editing, Writing – original draft, Investigation, Conceptualization. **Alexander Birich:** Writing – review & editing, Resources, Investigation, Funding acquisition. **Stefan Salhofer:** Writing – review & editing, Investigation, Funding acquisition, Conceptualization.

Declaration of competing interest

The authors declare that they have no known competing financial interests or personal relationships that could have appeared to influence the work reported in this paper.

Acknowledgments

This publication was partially supported by the Volkswagen Stiftung through the project "ShortCircuits - Development of a small-scale processing route for the localised short-loop recycling of waste electronic circuit boards," in line with the approved funding framework.

Supplementary materials

Supplementary material associated with this article can be found, in the online version, at doi:10.1016/j.resconrec.2025.108741.

Data availability

Data will be made available on request.

References

Bieler, T.R., Lee, T.K., 2017. Lead-free solder. Reference Module in Materials Science and Materials Engineering. Elsevier.

Bonov, P., 2018. Weekly poll results: the ideal weight for a phone is between 140g and 170g https://www.gsmarena.com/weekly_poll_results_the_ideal_weight_for_a_phone_is_between_140g_and_170g-news-29934.php. (Accessed 05.03.2025.

Bookhagen, B., Bastian, D., Buchholz, P., Faulstich, M., Opper, C., Irrgeher, J., Prohaska, T., Koeberl, C., 2020. Metallic resources in smartphones. Resour. Policy 68, 101750.

Bookhagen, B., Obermaier, W., Opper, C., Koeberl, C., Hofmann, T., Prohaska, T., Irrgeher, J., 2018. Development of a versatile analytical protocol for the comprehensive determination of the elemental composition of smartphone compartments on the example of printed circuit boards. Anal. Methods 10 (31), 3864–3871.

Bruno, M., Sotera, L., Fiore, S., 2022. Analysis of the influence of mobile phones' material composition on the economic profitability of their manual dismantling. J. Environ. Manage. 309, 114677.

Buczkó, N.A., Maróti, B., Gméling, K., Szentmiklósi, L., 2024. Neutron-based analytical techniques for the elemental composition analysis of electronic waste samples: advantages and challenges. J. Radioanal. Nucl. Chem. 333 (10), 5135–5150.

Cesaro, A., Belgiorno, V., Gorrasi, G., Viscusi, G., Vaccari, M., Vinti, G., Jandric, A., Dias, M.I., Hursthouse, A., Salhofer, S., 2019. A relative risk assessment of the open burning of WEEE. Environ. Sci. Pollut. Res. 26 (11), 11042–11052.

Chen, Z., Yang, M., Shi, Q., Kuang, X., Qi, H.J., Wang, T., 2019. Recycling waste circuit board efficiently and environmentally friendly through small-molecule assisted dissolution. Sci. Rep. 9 (1), 17902.

D'Adamo, I., Ferella, F., Gastaldi, M., Maggiore, F., Rosa, P., Terzi, S., 2019. Towards sustainable recycling processes: wasted printed circuit boards as a source of economic opportunities. Resour. Conserv. Recycl. 149, 455–467.

DOWA, 2024. E-scrap recycling. https://www.dowa-eco.co.jp/en/service/e-scrap-recycling.html. (Accessed 20.02.2025.

ELEPCB, 2024. Mobile PCB board. https://www.elepcb.com/blog/mobile-pcb-board/?utm_source=chatgpt.com.

Elmannai, W., Elleithy, K., Benz, A.A., DeAngelis, A.C., Weaver, N., 2023. An enhanced piezoelectric-generated power technique for Qi wireless charging. Clean Technol. 5 (1), 94–115.

Fontana, D., Pietrantonio, M., Pucciarmati, S., Rao, C., Forte, F., 2019. A comprehensive characterization of end-of-life mobile phones for secondary material resources identification. Waste Manag. 99, 22–30.

Geyer, R., Doctori Blass, V., 2010. The economics of cell phone reuse and recycling. Int. J. Adv. Manuf. Technol. 47 (5), 515–525.

Gómez, M., Grimes, S., Qian, Y., Feng, Y., Fowler, G., 2023. Critical and strategic metals in mobile phones: a detailed characterisation of multigenerational waste mobile phones and the economic drivers for recovery of metal value. J. Clean Prod. 419, 138099.

Gorewoda, T., Eschen, M., Charasińska, J., Knapik, M., Kozłowicz, S., Anyszkiewicz, J., Jadwiński, M., Potempa, M., Gawliczek, M., Chmielarz, A., Kurylak, W., 2020. Determination of metals' content in components mounted on printed circuit boards from end-of-life mobile phones. Recycling 5 (3), 4–7.

Gupta, N., Trivedi, A., Hait, S., 2021. Material composition and associated toxicological impact assessment of mobile phones. J. Environ. Chem. Eng. 9 (1), 104603.

Hagelüken, C., 2006. Recycling of Electronic Scrap At Umicore's Integrated Metals Smelter and Refinery. World of Metallurgy - ERZMETALL.

Holgersson, S., Steenari, B.-M., Björkman, M., Cullbrand, K., 2018. Analysis of the metal content of small-size Waste Electric and Electronic Equipment (WEEE) printed circuit boards—Part 1: internet routers, mobile phones and smartphones. Resour. Conserv. Recycl. 133, 300–308.

Ichikawa, S., Hirokawa, Y., Kurisaki, T., Nakamura, T., 2023. Characterization of a printed-circuit board by X-ray fluorescence and X-ray diffraction analyses for metal recovery. Spectrochim. Acta Part B Atom. Spectrosc. 210, 106819.

Ippolito, N.M., Belardi, G., Innocenzi, V., Medici, F., Pietrelli, L., Piga, L., 2021. Smart determination of gold content in PCBs of waste mobile phones by coupling of XRF and AAS techniques. Processes 9 (9), 3.

ITU, 2024. Mobile Cellular Subscriptions. https://data.worldbank.org/indicator/IT.CEL.SETS?end=2023&start=1995&view=chart. 2025).

Jandric, A., Zafiu, C., Hermann, G., Salhofer, S., 2024. A novel calibration method for portable X-ray fluorescence analysis of printed circuit boards. (1096-3669 (Electronic)).

JCGM, 2010. Evaluation of measurement data — Guide to the expression of uncertainty in measurement, OIML G 1-100 Edition 2008 ed.

Kamczyc, A., 2021. Electronic scrap processors see profits, despite decline in precious metals. https://www.recyclingtoday.com/news/electronic-scrap-precious-metals/?utm_source=chatgpt.com. (Accessed 20.02.2025.

Kasper, A.C., Berselli, G.B., Freitas, B.D., Tenorio, J.A., Bernardes, A.M., Veit, H.M., 2011. Printed wiring boards for mobile phones: characterization and recycling of copper. Waste Manag. 31 (12), 2536–2545.

Khaliq, A., Rhamdhani, M.A., Brooks, G., Masood, S., 2014. Metal extraction processes for electronic waste and existing industrial routes: a review and Australian perspective. Resources 3 (1), 152–179.

Kim, S., Lee, W., Park, J., 2022. A 2-DOF impact actuator for haptic application. Actuators 11 (3), 70.

Korf, N., Løvik, A.N., Figi, R., Schreiner, C., Kuntz, C., Mählitz, P.M., Rösslein, M., Wäger, P., Rotter, V.S., 2019. Multi-element chemical analysis of printed circuit boards – challenges and pitfalls. Waste Manag. 92, 124–136.

Kumari, R., Samadder, S.R., 2023. Evaluation of the recycling potential of obsolete mobile phones through secondary material resources identification: a comprehensive characterization study. J. Environ. Manage. 345, 118550.

Lancaster, S.T., Sahlin, E., Oelze, M., Ostermann, M., Vogl, J., Laperche, V., Touze, S., Ghestem, J.-P., Dalencourt, C., Gendre, R., Stammeier, J., Klein, O., Pröfrock, D., Košarac, G., Jotanovic, A., Bergamaschi, L., Di Luzio, M., D'Agostino, G., Jaćimović, R., Eberhard, M., Feiner, L., Trimmel, S., Rachetti, A., Sara-Aho, T., Roethke, A., Michaliszyn, L., Pramann, A., Rienitz, O., Irrgeher, J., 2024. Evaluation of X-ray fluorescence for analysing critical elements in three electronic waste matrices: a comprehensive comparison of analytical techniques. Waste Manag. 190, 496–505.

Lennartsson, A., Engström, F., Samuelsson, C., Björkman, B., Pettersson, J., 2018. Large-scale WEEE recycling integrated in an ore-based Cu-extraction system. J. Sustain. Metall. 4 (2), 222–232.

Liu, K., Tan, Q., Yu, J., Wang, M., 2023. A global perspective on e-waste recycling. Circ. Econ. 2 (1), 100028.

Liu, Y., Zhang, L., Song, Q., Xu, Z., 2020. Recovery of palladium and silver from waste multilayer ceramic capacitors by eutectic capture process of copper and mechanism analysis. J. Hazard. Mater. 388, 122008.

Maurice, A.A., Dinh, K.N., Charpentier, N.M., Brambilla, A., Gabriel, J.-C.P., 2021. Dismantling of printed circuit boards enabling electronic components sorting and their subsequent treatment open improved elemental sustainability opportunities. Sustainability 13 (18), 10357.

Naka, M., 2006. International recycling network of mobile phone in Asia Region. DOWA Eco-System.

Nolte, A., 2018. Metals For Progress – Nachhaltige Multi-Metall-Gewinnung bei Aurubis. Thomé-Kozmiensky Verlag GmbH.

Oguchi, M., Murakami, S., Sakanakura, H., Kida, A., Kameya, T., 2011. A preliminary categorization of end-of-life electrical and electronic equipment as secondary metal resources. Waste Manag. 31 (9–10), 2150–2160.
Oh, J.H., Kim, J.S., Moon, S.M., Min, J.W., 2012. Module of urban mining recycling technology and non-ferrous smelting process in Korea. J. Resour. Recycl. 21 (1), 3–16.
Otsuki, A., Mensbruge, L.D.L., King, A., Serranti, S., Fiore, L., Bonifazi, G., 2020. Non-destructive characterization of mechanically processed waste printed circuit boards - particle liberation analysis. Waste Manag. 102, 510–519.
Owusu-Sekyere, K., Aladago, D.A., Leverenz, D., Oteng-Ababio, M., Kranert, M., 2024. Environmental impacts on soil and groundwater of informal E-waste recycling processes in Ghana. Sustainability 16 (11), 4347.
Pawlek, F., 1983. Metallhüttenkunde. De Gruyter.
Perdigones, F., Quero, J.M., 2022. Printed circuit boards: the layers' functions for electronic and biomedical engineering. Micromachines 13 (3), 22.
Rao, M.D., Singh, K.K., Morrison, C.A., Love, J.B., 2021. Optimization of process parameters for the selective leaching of copper, nickel and isolation of gold from obsolete mobile phone PCBs. Clean. Eng. Technol. 4, 100180.
Rocchetti, L., Amato, A., Beolchini, F., 2018. Printed circuit board recycling: a patent review. J. Clean Prod. 178, 814–832.
Romano, P., Ippolito, N.M., Vegliò, F., 2023. Chemical characterization of an ARDUINO® board and its surface mount devices for the evaluation of their intrinsic economic value. Processes 11 (7), 1911.
Sahan, M., Kucuker, M.A., Demirel, B., Kuchta, K., Hursthouse, A.A.-O., 2019. Determination of metal content of waste mobile phones and estimation of their recovery potential in Turkey. LID - 10.3390/ijerph16050887 [doi] LID - 887. (1660-4601 (Electronic)).
Shearer, F., 2011. Power Management in Mobile Devices. Elsevier, Newnes.
Singh, N., Duan, H., Yin, F., Song, Q., Li, J., 2018. Characterizing the materials composition and recovery potential from waste mobile phones: a comparative evaluation of cellular and smart phones. ACS Sustain. Chem. Eng. 6 (10), 13016–13024.
Tantawi, O., Hua, I., 2021. Temporal evolution of metallic element composition and environmental impact in consumer electronic devices: a study of smartphones. Resour. Conserv. Recycl. 175, 105886.
Themelis, N.J., McKerrow, G.C., Tarassoff, P., Hallett, G.D., 1972. The Noranda process. Jom 24 (4), 25–32.
Vaccari, M., Vinti, G., Cesaro, A., Belgiorno, V., Salhofer, S., Dias, M.I., Jandric, A., 2019. WEEE treatment in developing countries: environmental pollution and health consequences-an overview. Int. J. Environ. Res. Public Health 16 (9), 1595.
Van Yken, J., Cheng, K.Y., Boxall, N.J., Sheedy, C., Nikoloski, A.N., Moheimani, N.R., Kaksonen, A.H., 2021. A comparison of methods for the characterisation of waste-printed circuit boards. Metals 11 (12), 1935 (Basel).
Workman, M.. Disassembling the dilemmas. Recycling Today. https://www.recyclingtoday.com/article/disassembling-the-dilemmas/.
Worldometers, 2025. Current world population. https://www.worldometers.info/world-population/. 2025).
Zhang, X., Qian, Q., Qiang, L., Zhang, B., Zhang, J., 2020. Comparison study of gold coatings prepared by traditional and modified galvanic replacement deposition for corrosion prevention of copper. Microelectr. Reliab. 110, 113695.
Zhao, C., Zhang, X., Ding, J., Zhu, Y., 2017. Study on recovery of valuable metals from waste mobile phone PCB particles using liquid-solid fluidization technique. Chem. Eng. J. 311, 217–226.